Use of Magnetization Phase in Applications - 2

O. Wieben, Ph.D.
owieben@wisc.edu
Depts. of Medical Physics & Radiology
University of Wisconsin - Madison

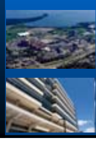

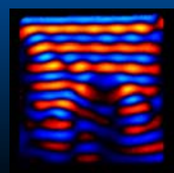

Chemical Shift Imaging

Separate metabolites with different chemical shifts, e.g.

- Fat / Water Seperation for Fat Suppression or Fat Quantification
- Metabolite maps for hyperpolarized gas imaging (13C) for Lactate, Alanin, and Pyruvate

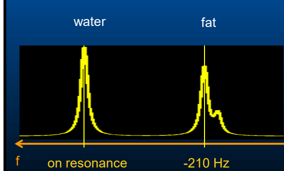

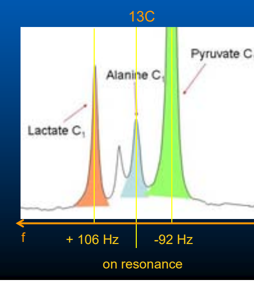

Chemical Shift Imaging

MR Spectroscopy

- High spectral information, low spatial information, long scan times
- No a priori information exploited

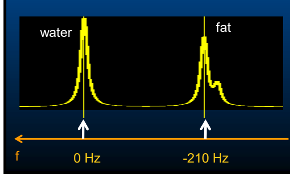

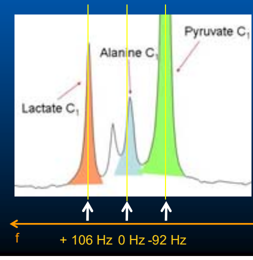

MR Spectroscopy

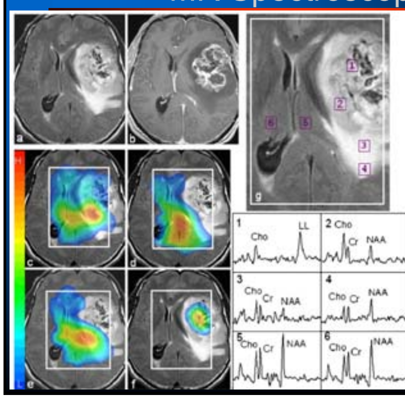

PRESS acquistion
2D multivoxel 1H-MRSI
32x32 voxels zerofilled
scan time: 6min53s

a: FLAIR
b: CE T1weighted

Maps:
c: Choline map
d: N-acetylaspatate
e: Creatine (Cr)
f: Lactate / Lipids

A Di Costanzo et al.
Eur Radiol 2007

Fig. 1 Example of 2D-multivoxel proton spectroscopic imaging (^{1}H-MRSI) performed using a 3.0-T MR scanner (Signa Horizon LX) with a standard head coil, and the protocol (PROBE/SI) and the software (Functool Performance) provided by the manufacturer (General Electric Medical Systems, Milwaukee, WI). In brief, a point-resolved spectroscopy (PRESS) pulse sequence, with repetition time (TR) 1,500 ms, echo time (TE) 144 ms, field of view (FOV) 24 cm, phase 16, section thickness 10 mm and acquisition time 6 min 53 s, provided a spectroscopic data set, which was spatially zerofilled to 32×32 images with a final voxel resolution of 7.5×7.5×10 mm (0.56 cm^3). Fluid-attenuated inversion recovery (FLAIR) (**a**) and contrast-enhanced T_1-weighted (**b**) images from a 45-year-old man with a left fronto-temporo-parietal glioblastoma. Choline (Cho) (**c**), N-acetylaspartate (NAA) (**d**), creatine (Cr) (**e**) and lactate/lipids (LL) (**f**) maps. Localizing FLAIR image (**g**) and spectra (**1–6**) from the corresponding boxes in **g**. Color scale: *red* strongest signal intensity; *blue* weakest signal intensity. Higher spatial resolution improves the ability to recognize the spatial heterogeneity of high-grade gliomas. The spectrum **1**, showing a low level of Cho, undetectability of Cr and NAA, and high LL peak, suggests the presence of necrosis. The spectrum **2**, in the margins of glioma, presents the typical tumor pattern, characterized by an abnormal Cho/NAA ratio (<1). The spectra **3** and **4**, in an apparently edematous region surrounding the enhanced margins of glioma, show low metabolite levels, as compared to the normal spectra **5** and **6**, but different pattern: the spectrum **3** has a tumor pattern and suggests the presence of infiltrating tumor cells; the spectrum **4** has a normal Cho/NAA ratio and suggests noninfiltrated vasogenic edema

A Di Costanzo et al.
Eur Radiol 2007

MR-Signal Phase | *Chemical Shift*

- Fat-water difference = 220 Hz @ 1.5T / 440 Hz @ 3T
- Displacement fat vs. water ➔ Misregistration

1 pixel = 2*BW/matrix Hz

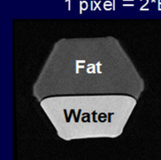

BW = 6.94kHz
➔ 4 pixel shift

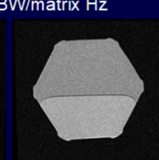

BW = 31.25kHz
➔ 0.9 pixel shift

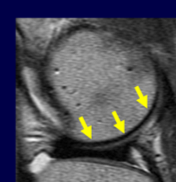

BW = 9.23kHz
➔ 3 pixel shift

Degree of misregistration { - Bandwidth
- Field strength

Solving for ‚arbitrary‘ TE‘s

$$\hat{s}(t_n) = \left(\underline{\hat{\rho}_w} e^{-j2\pi\Delta f_w t_n} + \underline{\hat{\rho}_f} e^{-j2\pi\Delta f_f t_n}\right) e^{-j2\pi\underline{\psi} t_n}$$

5 unknowns: 2×complex
1×scalar

Simple solution: Fieldmap=0 -> Matrix Inversion

Matrix Notation: $\hat{\mathbf{S}} = \mathbf{A}\,\hat{\boldsymbol{\rho}}$

Better solution: iterative approach

- estimate field map ΔB_0
- no phase unwrapping required
- ‘free choice‘ of TR und ΔTE

Fat Water Separation with IDEAL

SB Reeder, MRM, 2004

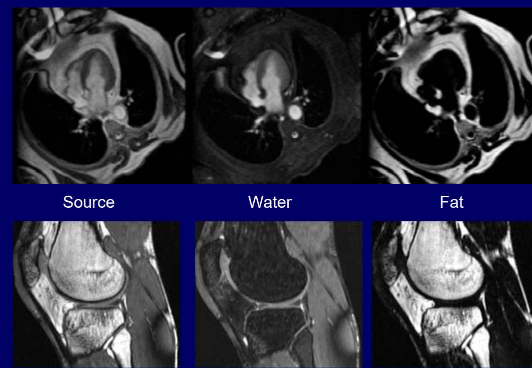

Multiecho GRE

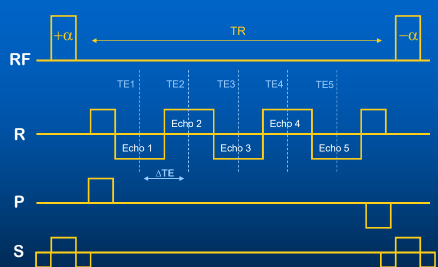

O Wieben et al., ISMRM 2005, p. 2386

EPSI – Timing Properties

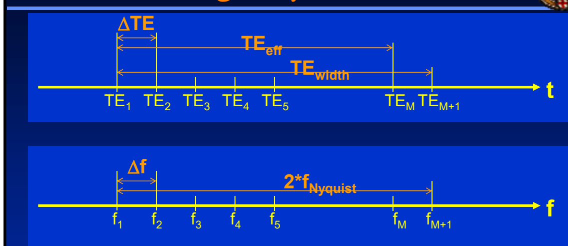

$f_{Nyquist} = 1 / (2^*\Delta TE)$

$\Delta f = 2^*f_{Nyquist} / M = 1 / (\Delta TE^*M) = 1 / TE_{width}$

$TE_{eff} = \Delta TE^*(M-1)$

EPSI – Proof of principle

Proof of principle

FLASH images (no need for ultrashort TR)

Single echo measurements (no ‘EPI problems’)

3 components

- **Water – Acetone - Fat**

Imaging Sequence

- **TR = 40 ms**
- **20 Echos: 5 ms <= Te <= 4 ms**
- **ΔT = 1 ms -> $f_{Nyquist}$ = 500 Hz**
- **T_{width} = 20 ms -> Δf = 50 Hz**

Daten vom 28 Jan 04 - SPGR

SPGR – Mag and Phase

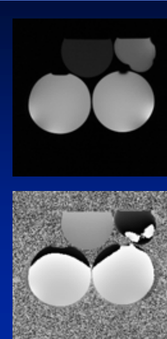

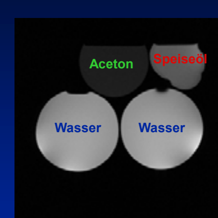

T_{width} = 20ms, ΔTE = 1 ms
-> Δf = 50 Hz, $f_{Nyquist}$ = 500

Daten vom 28 Jan 04 - SPGR

SPGR – Phase vs. TE

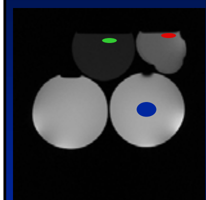

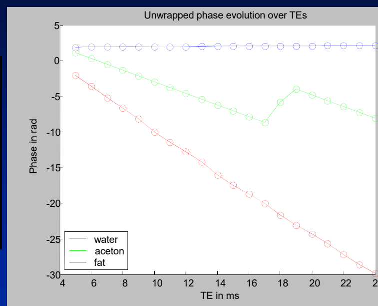

Daten vom 28 Jan 04 - SPGR

SPGR – Frequency Spectrum

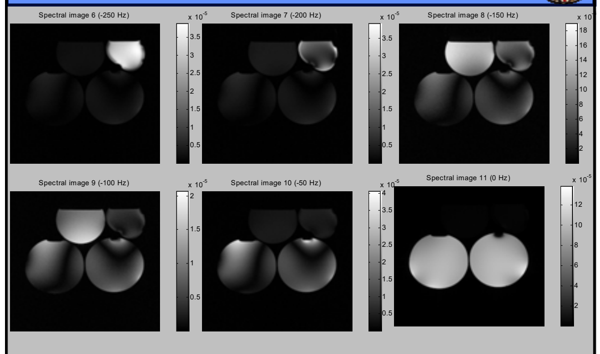

Daten vom 28 Jan 04 - SPGR

SPGR – Frequency Spectrum

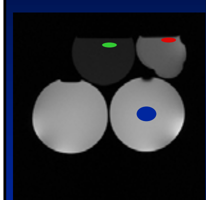

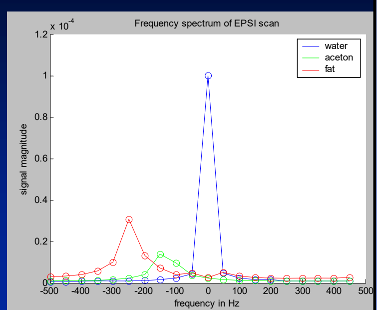

Daten vom 28 Jan 04 - SPGR

Fat – multi peaks

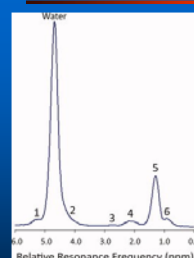

Figure 1. Fatty liver spectrum in a 44-year-old woman with fatty liver disease. An MR spectrum was acquired from a single 20 × 20 × 20 mm³ voxel in the right lobe during a single breath-hold without averaging using the STEAM sequence at 3T (TR/TE = 3500/10 msec; mixing time = 5 msec). Six distinct fat peaks can be resolved in vivo at clinical field strengths, as labeled (1–6), corresponding to the peaks in Table 1.

Table 1
Proton MR Spectrum of Liver Triglycerides

Peak	In vivo ppm	Ex vivo ppm	Chemical environment	Type	Relative magnitude
1	5.3	5.29	-CH=CH-	Olefinic	4.7%
		5.19	-CH-O-CO-	Glycerol	
Water	4.7	4.70	H_2O	—	—
2	4.2	4.20	$-CH_2-O-CO-$	Glycerol	3.9%
3	2.75	2.75	$-CH=CH-CH_2-CH=CH-$	Diacyl	0.6%
4	2.1	2.24	$-CO-CH_2-CH_2-$	α-Carboxyl	12.0%
		2.02	$-CH_2-CH=CH-CH_2-$	α-Olefinic	
5	1.3	1.60	$-CO-CH_2-CH_2-$	β-Carboxyl	0.7
		1.30	$-(CH_2)_n-$	Methylene	
6	0.9	0.9	$-(CH_2)_n-CH_3$	Methyl	0.088

Proton MR spectrum of liver fat measured by Hamilton et al (84). The different liver fat proton moieties (bold H) produce nine resonances ex vivo at high field strength. In vivo, at clinical field strengths, these resonances are resolvable into six distinct fat peaks, though peaks 1 and 2 cannot be clearly distinguished from water. The liver spectrum can be used to correct for fat peaks included in water in MRS, as well as spectral modeling used in advanced imaging techniques (60,63,76,82,85). The relative magnitudes listed may not apply to other fat deposits.

Reeder et al, Journal of Magnetic Resonance Imaging
Volume 34, Issue 4, pages 729-749, 16 SEP 2011

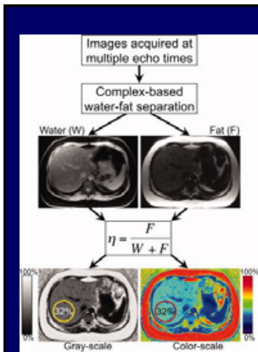

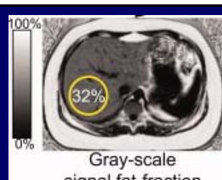

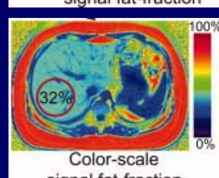

Quantitative assessment of liver fat with magnetic resonance imaging and spectroscopy

Journal of Magnetic Resonance Imaging
Volume 34, Issue 4, pages 729-749, 16 SEP 2011 DOI: 10.1002/jmri.22580
http://onlinelibrary.wiley.com/doi/10.1002/jmri.22580/full#fig4

Velocity Mapping

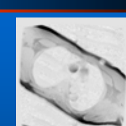

Background

- Assessment of blood flow & tissue motion
  - → Evaluation of regional cardiovascular function

Concept: Velocity Encoding

- Exploit sensitivity of MR-signal phase to flow / motion
  - ➔ Phase shifts for moving spins

- **Bipolar gradients**
  - ➔ Encoding of local blood flow / tissue motion

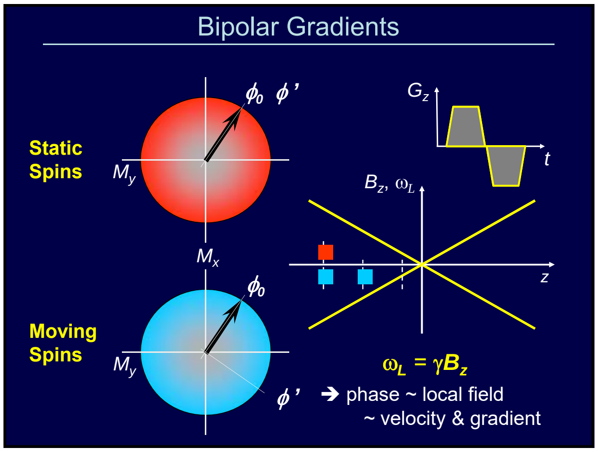
Bipolar Gradients
Static Spins
Moving Spins
ϕ_0 ϕ'
M_y
M_x
G_z
t
B_z, ω_L
z
$\omega_L = \gamma B_z$
➔ phase ~ local field
~ velocity & gradient

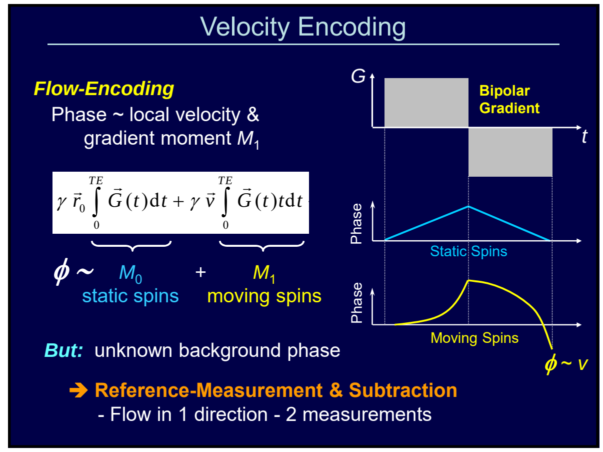
Velocity Encoding
Flow-Encoding
Phase ~ local velocity &
gradient moment M_1
$\gamma \vec{r}_0 \int_0^{TE} \vec{G}(t)dt + \gamma \vec{v} \int_0^{TE} \vec{G}(t)tdt$
$\phi \sim$ M_0 + M_1
static spins
moving spins
But: unknown background phase
➔ Reference-Measurement & Subtraction
- Flow in 1 direction - 2 measurements
G
Bipolar Gradient
t
Phase
Static Spins
Moving Spins
$\phi \sim v$

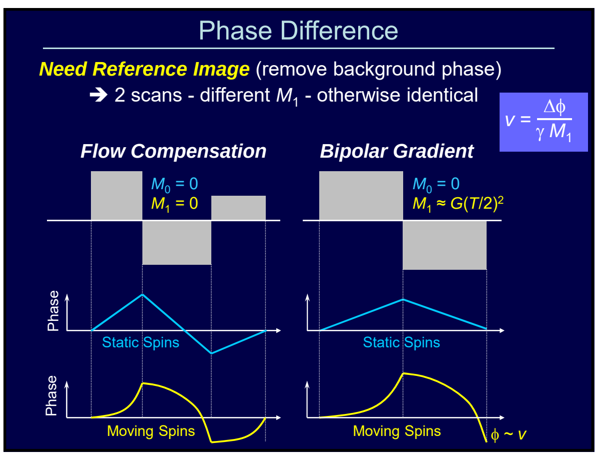
Phase Difference
Need Reference Image (remove background phase)
➔ 2 scans - different M_1 - otherwise identical
$v = \frac{\Delta\phi}{\gamma M_1}$
Flow Compensation
Bipolar Gradient
$M_0 = 0$
$M_1 = 0$
$M_0 = 0$
$M_1 \approx G(T/2)^2$
Phase
Static Spins
Moving Spins
$\phi \sim v$

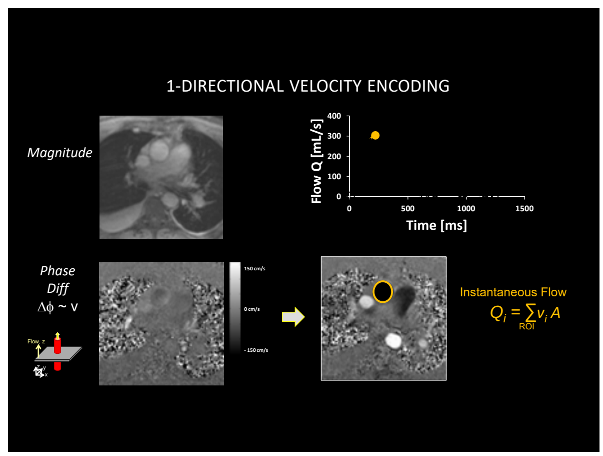
1-DIRECTIONAL VELOCITY ENCODING
Magnitude
Flow Q [mL/s]
Time [ms]
Phase
Diff
$\Delta\phi \sim v$
Instantaneous Flow
$Q_i = \sum_{ROI} v_i A$

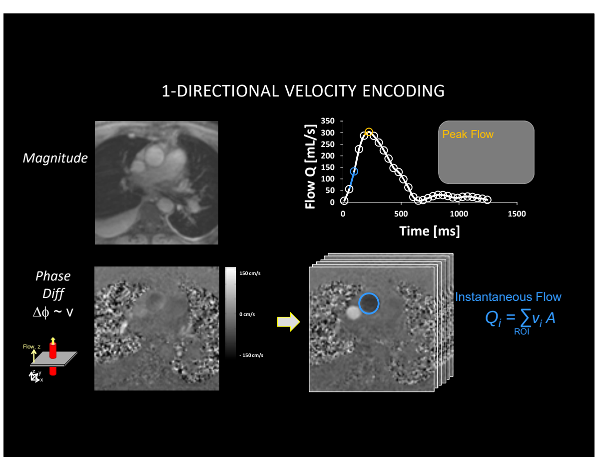
1-DIRECTIONAL VELOCITY ENCODING
Magnitude
Flow Q [mL/s]
Time [ms]
Peak Flow
Phase
Diff
$\Delta\phi \sim v$
Instantaneous Flow
$Q_i = \sum_{ROI} v_i A$

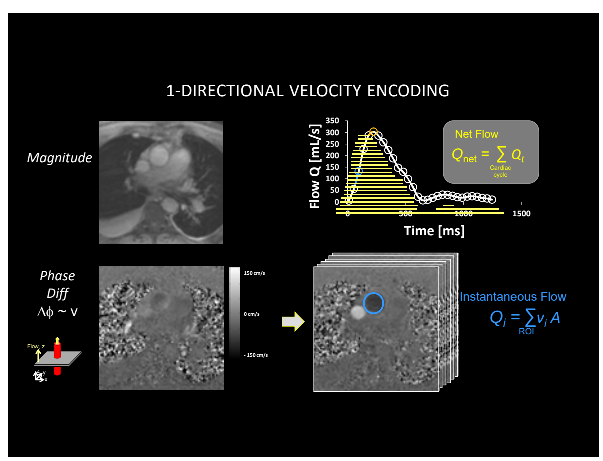
1-DIRECTIONAL VELOCITY ENCODING
Magnitude
Flow Q [mL/s]
Time [ms]
Net Flow
$Q_{net} = \sum_{Cardiac\ cycle} Q_i$
Phase
Diff
$\Delta\phi \sim v$
Instantaneous Flow
$Q_i = \sum_{ROI} v_i A$

1-Directional Velocity Encoding

ECG gated, velocities encoded in phase difference image $\Delta\phi$

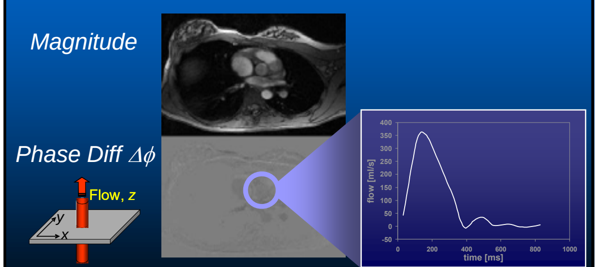

1-Directional Velocity Encoding

ECG gated, velocities encoded in phase difference image $\Delta\phi$

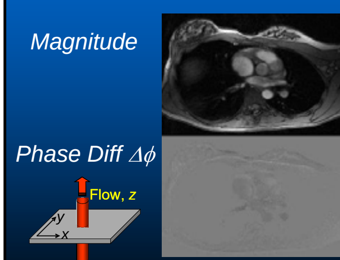

Desired parameters
Single slice
Readout: 256
# of phase encodes: 160
TR = 8 ms
Views per segment = 6
Temporal resolution = 48 ms
Heart rate = 60 bpm
# of cardiac phases: 20

Scan duration
160/6 * 2 = 54 heart beats
= 54 s
-> shorten scan time to single breath hold!
view sharing
partial Fourier
parallel imaging
...

Common Applications

Heart & Great Vessels (breath hold)
- Cardiac output
- Regurgitation volumes (valves)
- Valve insuffiency
- Stenoses
- Coarctation
- ...

Neurovascular
- Carotid arteries and others

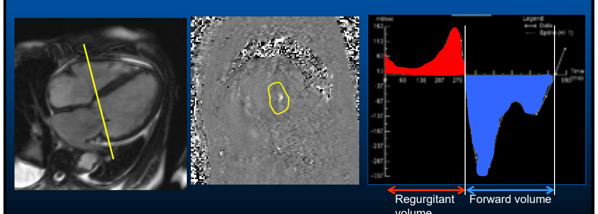

C. Francois , University of Wisconsin

Common Applications

Heart & Great Vessels (breath hold)
- Cardiac output
- Regurgitation volumes (valves)
- Valve insuffiency
- Stenoses
- Coarctation
- ...

Neurovascular
- Carotid arteries and others

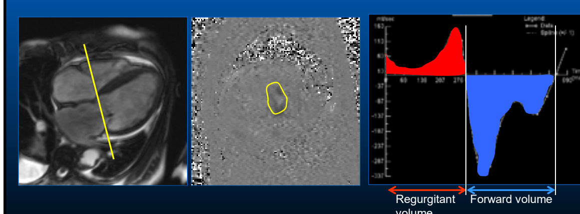

C. Francois , University of Wisconsin

3-Directional Velocity Encoding

Acquire four data sets:

(1) with flow comp

(2) with flow in slice

(3) with flow in phase

(4) with flow in read

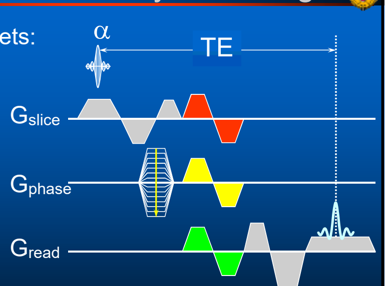

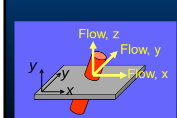

Courtesy of Klaus Scheffler, University of Basel

Volumetric 3-directional PC MRI

Acquisition
- Volumetric coverage
- 3-directional flow encoding: 4 acquisitions
- ECG gating
- Breathing motion in abdomen and chest

Reduce acquisition times
- View sharing & advanced resp gating *M Markl et al., JMRI 2003*
- Radial undersampling (PC VIPR) *TL Gu et al., AJNR 2005*
- kt BLAST *C Baltes et al., MRM 2005*
- ...

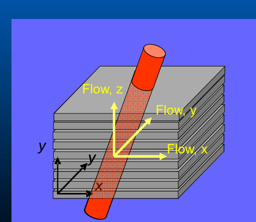

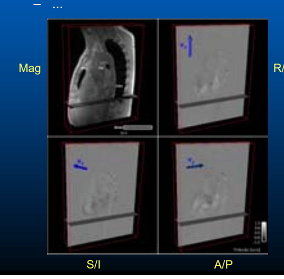

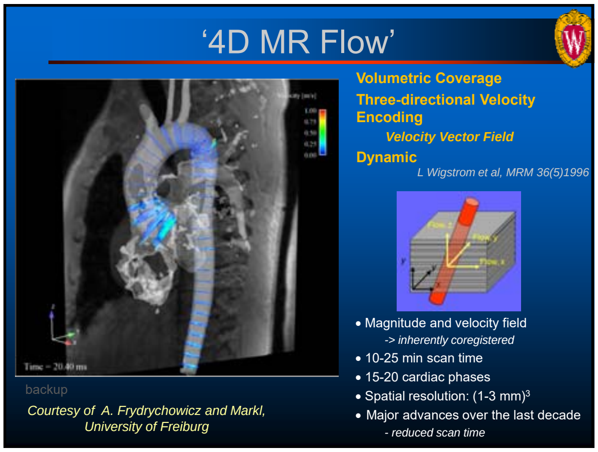
'4D MR Flow'
Volumetric Coverage
Three-directional Velocity Encoding
Velocity Vector Field
Dynamic
L Wigstrom et al, MRM 36(5)1996
• Magnitude and velocity field
-> inherently coregistered
• 10-25 min scan time
• 15-20 cardiac phases
• Spatial resolution: (1-3 mm)³
• Major advances over the last decade
- reduced scan time
backup
Courtesy of A. Frydrychowicz and Markl,
University of Freiburg

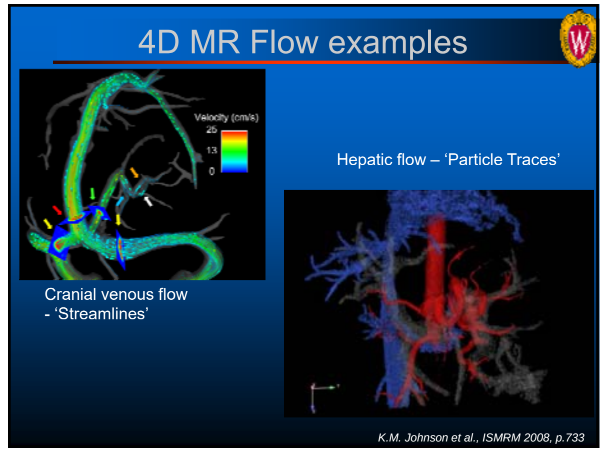
4D MR Flow examples
Velocity (cm/s)
25
13
0
Cranial venous flow
- 'Streamlines'
Hepatic flow – 'Particle Traces'
K.M. Johnson et al., ISMRM 2008, p.733

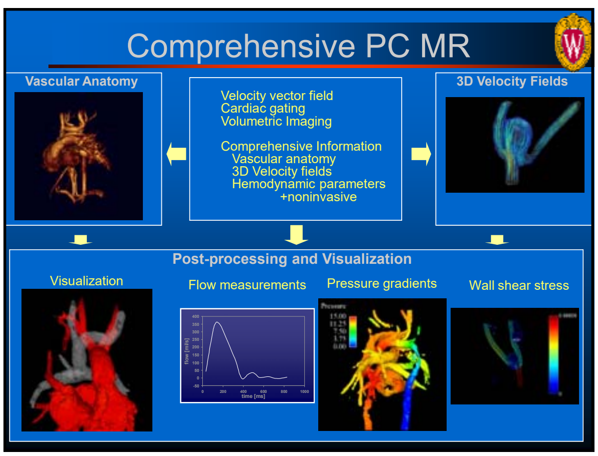
Comprehensive PC MR
Vascular Anatomy
Velocity vector field
Cardiac gating
Volumetric Imaging
Comprehensive Information
Vascular anatomy
3D Velocity fields
Hemodynamic parameters
+noninvasive
3D Velocity Fields
Post-processing and Visualization
Visualization
Flow measurements
Pressure gradients
Wall shear stress

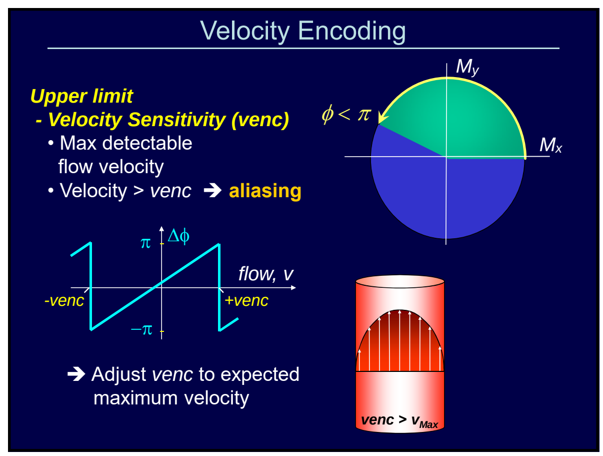
Velocity Encoding
Upper limit
- Velocity Sensitivity (venc)
• Max detectable flow velocity
• Velocity > venc ➔ aliasing
$\phi < \pi$
M_y
M_x
π
$\Delta\phi$
flow, v
-venc
+venc
$-\pi$
➔ Adjust venc to expected maximum velocity
venc > v_{Max}

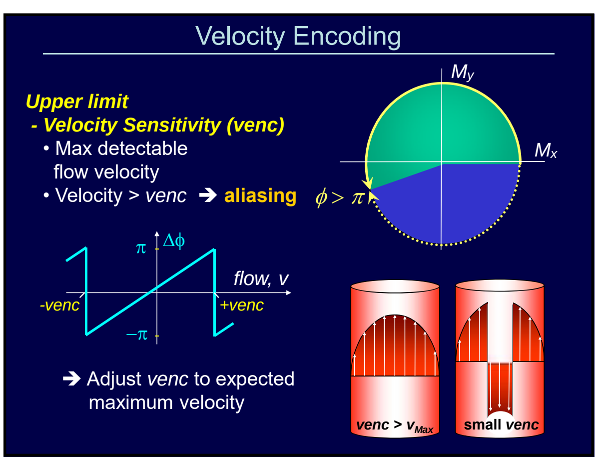
Velocity Encoding
Upper limit
- Velocity Sensitivity (venc)
• Max detectable flow velocity
• Velocity > venc ➔ aliasing
$\phi > \pi$
M_y
M_x
π
$\Delta\phi$
flow, v
-venc
+venc
$-\pi$
➔ Adjust venc to expected maximum velocity
venc > v_{Max}
small venc

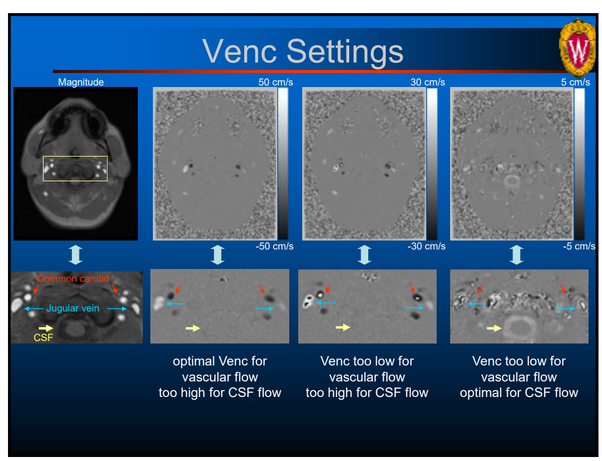
Venc Settings
Magnitude
50 cm/s
30 cm/s
5 cm/s
-50 cm/s
-30 cm/s
-5 cm/s
Common carotid
Jugular vein
CSF
optimal Venc for vascular flow
too high for CSF flow
Venc too low for vascular flow
too high for CSF flow
Venc too low for vascular flow
optimal for CSF flow

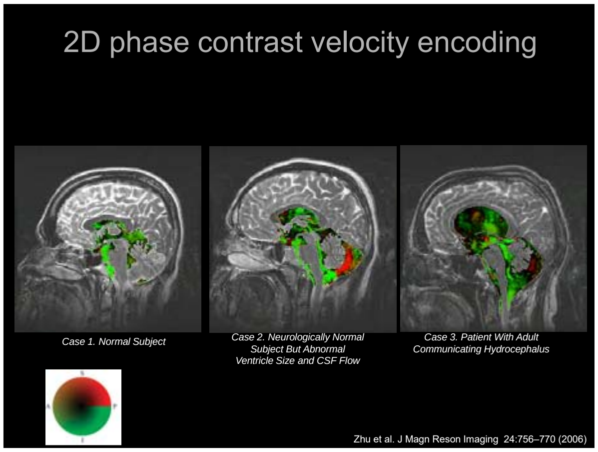
2D phase contrast velocity encoding
Case 1. Normal Subject
Case 2. Neurologically Normal Subject But Abnormal Ventricle Size and CSF Flow
Case 3. Patient With Adult Communicating Hydrocephalus
Zhu et al. J Magn Reson Imaging 24:756–770 (2006)

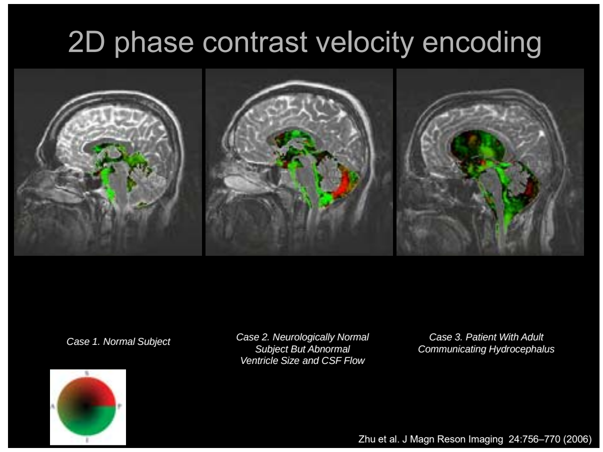
2D phase contrast velocity encoding
Case 1. Normal Subject
Case 2. Neurologically Normal Subject But Abnormal Ventricle Size and CSF Flow
Case 3. Patient With Adult Communicating Hydrocephalus
Zhu et al. J Magn Reson Imaging 24:756–770 (2006)